frontiers | Frontiers in Environmental Science

ORIGINAL RESEARCH
published: 25 May 2022
doi: 10.3389/fenvs.2022.852673

Subseasonal Reversal of Winter Temperature Over Northeast China in 2014/2015: Role of Arctic Sea Ice

Haixia Dai[1] *and Ke Fan*[2]*

[1]Key Laboratory of Polar Science, MNR, Polar Research Institute of China, Shanghai, China, [2]School of Atmospheric Sciences, Sun Yat-sen University, and Southern Marine Science and Engineering Guangdong Laboratory (Zhuhai), Zhuhai, China

This study investigates the temperature reversal over Northeast China (NEC) in winter 2014/2015, focusing on the variations of related general circulations and the affecting mechanisms of the Arctic sea ice on daily scale. It turns out to be the coupled impacts of the eastward propagations of tropospheric wave trains from the North Atlantic Ocean and the downward reflections of planetary wavenumber-1 from the stratosphere that resulted in the subseasonal reversal of winter temperature over NEC in winter 2014/2015. Also, such anomalous atmospheric circulations can be attributed to sea-ice anomalies over the Davis Strait–Baffin Bay (SIC-DSBB) and the Barents–Kara Sea (SIC-BKS) in November 2014. SIC-DSBB anomalies in November 2014 excited the eastward propagation of Rossby waves via the tripole pattern of sea surface temperature over the North Atlantic Sea, leading to the colder condition over NEC in the first and middle 10 days of December 2014. Anomalously heavy SIC-BKS also triggered wave trains from the polar region to Eurasia, strengthening the Rossby wave induced by SIC-DSBB. Moreover, the wave trains suppressed the upward propagation of planetary wavenumber-1 over the Siberia region, strengthening the stratospheric polar vortex. However, the sea-ice anomalies over these two domains only existed in November 2014. Thus, the tropospheric mechanisms by which the Arctic sea ice affected the temperature over NEC only lasted to late December 2014. Meanwhile, the stratospheric anomalies propagated downwards with the planetary wavenumber-1, favoring the positive phase of Arctic Oscillation in the troposphere and the warm condition over NEC since the last week of December 2014. Consequently, the temperature over NEC reversed in winter 2014/2015.

Keywords: Arctic sea ice, winter temperature, subseasonal reversal, Northeast China, daily scale

OPEN ACCESS

Edited by:
Yang Gao,
Ocean University of China, China

Reviewed by:
Shangfeng Chen,
Institute of Atmospheric Physics (CAS), China
Botao Zhou,
Nanjing University of Information Science and Technology, China

***Correspondence:**
Ke Fan
fank8@mail.sysu.edu.cn

Specialty section:
This article was submitted to Atmosphere and Climate, a section of the journal Frontiers in Environmental Science

Received: *11 January 2022*
Accepted: *28 April 2022*
Published: *25 May 2022*

Citation:
Dai H and Fan K (2022) Subseasonal Reversal of Winter Temperature Over Northeast China in 2014/2015: Role of Arctic Sea Ice. Front. Environ. Sci. 10:852673. doi: 10.3389/fenvs.2022.852673

INTRODUCTION

The temperature over China features both spatial variations and significant intraseasonal variability (Shao, 2014; Li and Tan, 2020). Spatially, the winter temperature of China exhibits leading modes as a homogeneous variation or north–south dipole pattern on the interannual time scale (Kang et al., 2009). Temporally, the winter temperature over China features three formations on the subseasonal scale, like opposite patterns between the prophase and anaphase of the winter and alternations between cold and warm (Sun et al., 2019). Moreover, the cold waves can induce extreme events on the subseasonal scale, which have substantial impacts on socioeconomics, agricultural production, and

human life. Thus, it is essential to investigate the factors and physical mechanisms related to the evolution of cold waves invading China.

Previous studies have documented that intraseasonal oscillations exist over both the tropics and mid–high-latitude regions (Anderson and Rosen, 1983; Krishnamurti and Gadgil, 1985). The intraseasonal oscillations over the mid–high latitudes are independent of tropical forcing (Knutson and Weickmann, 1987; Ghil and Mo, 1991) and propagate southeastwards in boreal winter with the main periodicity being 10–30 days, inducing the intraseasonal variations of winter temperature over Eurasia (Yang and Li, 2016; Yang et al., 2019). Studies have pointed out that the winter temperature over China mainly features 10–20- and 30–60-days low-frequency oscillations with regional differences and annual variations (Jin and Sun, 1996; Liu et al., 2016; Li and Tan, 2020), and the intraseasonal signals could be attributable to the low-frequency oscillations of wave trains over the Eurasian mid–high-latitude region (Yang et al., 2014; Jiao et al., 2019). As a critical pattern of the atmospheric circulations over the Northern Hemisphere, the intraseasonal oscillations of the Arctic Oscillation (AO) induce the subseasonal variations of winter temperature over China by stimulating Rossby waves in the midlatitudes, thereby causing a meridional shift of cold air and modulating the high-frequency components of the Siberian high (Gong and Ho, 2004; Yao et al., 2016). Moreover, the tropical intraseasonal oscillation, the Madden–Julian Oscillation, can also influence winter weather over East Asia via intraseasonal changes in local Hadley circulation (He et al., 2011; Huang et al., 2018; Huang et al., 2021), and the combined effects with different phases of the AO (Song and Wu, 2019a; b). The significant influence of low-frequency Rossby waves on upper-troposphere and synoptic transient eddies in affecting the intraseasonal variations of the Siberian high and East Asian trough (EAT) have been revealed, which further impact the surface temperature over East Asia (Takaya and Nakamura, 2005a; Takaya and Nakamura, 2005b; Song et al., 2016). Furthermore, the intraseasonal signals in the stratosphere also contribute to the intensification of the Siberian high, EAT, and the occurrence of cold events over eastern China (Song et al., 2017).

Arctic sea ice, snow cover over Eurasia, and sea surface temperature (SST) over the North Pacific and the Indian Ocean all have considerable influences on the winter temperature over China on both seasonal and subseasonal scales. Wu and Chen (2015) documented the 3–5-days lagged relationship between intraseasonal SST variations in the South China Sea during boreal winter and the East Asian winter monsoon (EAWM) (Wu and Chen, 2015). The coupled intraseasonal variations of the EAWM and the South China Sea–western North Pacific SST were also investigated (Wu, 2015). The interactions of El Niño–Southern Oscillation (ENSO) events with the subtropical jet could cause a phase transition of the AO, which further leads to a subseasonal response of the Siberian high and cold-air intrusion from the polar region (Geng et al., 2017). A very recent study by Li et al. (2021) has also revealed the contributions of central Pacific ENSO to the temperature reversal of December and January over China. Besides SST, the Arctic sea ice also has essential effects on the subseasonal reversal of winter temperature in China. Lü et al. (2018) identified the mechanisms by which the autumn Arctic sea ice impact the intraseasonal reversal of the winter Siberian high. It was found that sea-ice anomalies impact the number of Ural blockings and the intensity of the westerlies via the storm track in northeastern Europe. The combined effects and mechanisms of Arctic sea ice over different regions on the temperature reversal of December and January–February over Northeast China (NEC) were also documented by Dai et al. (2019). Moreover, the noticeable subseasonal variations of snow cover over Eurasia also play a critical role in affecting the winter precipitation on the subseasonal scale, as well as the predictability of winter temperature over East Asia (Jeong et al., 2013; Ao and Sun, 2016; Li et al., 2020). The interactions between the Arctic sea ice and Siberian snow accumulation, and the related stratospheric processes, are also essential factors to cold events over Eurasia (Lü et al., 2020).

The EAWM was weaker than normal during winter 2014/2015, favoring a warm condition over China, especially in NEC (**Figure 1A**). However, the intensity of the EAWM featured a phase transition from strong to weak in winter 2014/2015, corresponding to the temperature reversal in China on the subseasonal scale (Wang et al., 2015). The modulation of the Niño4 SST anomalies by the positive-phase Pacific Decadal Oscillation and the effects of Arctic sea ice on winter temperature in China may have partly contributed to this event (Xu et al., 2018). The lagged influence of autumn Arctic sea ice on the weaker EAWM in winter 2014/2015 has also been noted (Xie et al., 2019). However, the explanation of the physical mechanism by which the Arctic sea ice influenced the phase transition of the EAWM remains inadequate. Although the influence of November Arctic sea ice on the temperature of NEC in December and January–February has been elucidated on the monthly scale (Dai et al., 2019), the evolutions of general circulations at the synoptic scale are still worthy of investigation. Previous studies have emphasized the importance of synoptic-scale transient wave activity and cold waves in affecting the winter climate over China (Ding and Krishnamurti, 1987; Qian and Zhang, 2007; Chen et al., 2012; Qian, 2012). Thus, further insight into the intraseasonal reversal of winter temperature over NEC could favor a better understanding of the related synoptic-scale evolutions of atmospheric circulations, the mechanisms, and the genesis, and provide a valuable reference for predictions at the subseasonal scale.

This paper carries out a further investigation of the temperature reversal event over NEC in winter 2014/2015 on the synoptic scale with the aim to identify the critical role of the Arctic sea ice.

DATA AND METHODS

Data

The station data used in this study are from the National Meteorological Information Center of China and contain the daily records of 824 gauge stations in China. A total of 68 out of 635 stations with no missing records during the period 1981–2021 are selected over NEC (42°–52°N, 120°–135°E). The daily observational atmospheric data are from the NCEP/NCAR reanalysis I dataset, including sea level pressure (SLP), geopotential height, zonal and

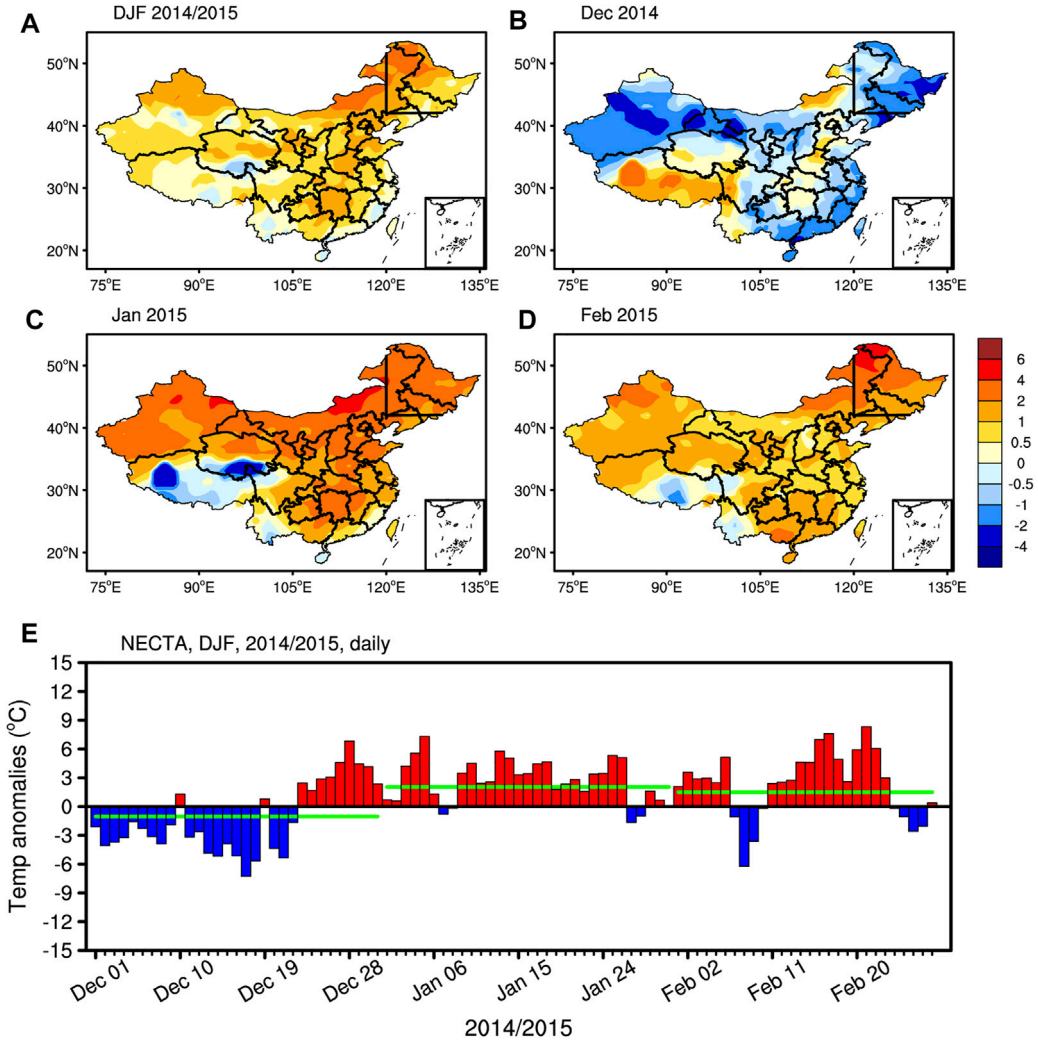

FIGURE 1 | Spatial pattern of **(A)** seasonally averaged and **(B–D)** monthly temperature (unit: °C) over China in winter 2014/2015. **(E)** Time series of daily temperature anomalies over NEC in winter 2014/2015. The black boxes in **(A–D)** denote the domain of NEC, and green lines in **(E)** indicate the monthly averaged values of temperature anomalies.

meridional wind, and surface air temperature with a horizontal resolution of 2.5° × 2.5°. The surface latent heat net flux and the surface sensible heat net flux are on a Gauss grid (Kalnay et al., 1996). The daily SST and the sea-ice cover (SIC) data are from the NOAA OISSTv2 dataset, with a horizontal resolution of 0.25° × 0.25° (Reynolds et al., 2007). Moreover, the daily AO index data are from the Climate Prediction Center (https://www.cpc.ncep.noaa.gov/products/precip/CWlink/daily_ao_index/ao.shtml).

Methods

The climatology is defined as the average span of the period 1980–2015. Several indices are employed to estimate the status of atmospheric or oceanic systems in this study, and the definitions are as follows:

The intensity of the Siberian high (SHI) is defined as the mean SLP averaged over the center of the anticyclone (40°–60°N, 70°–120°E) (Gong et al., 2001). The intensity of the EAT (EATSI) is represented by the averaged geopotential height at 500 hPa over (30°–45°N, 125°–145°E) (Sun and Li, 1997). The EAT axis index (EATAI) is calculated as the longitudinal position of the minimum 500 hPa height at each latitudinal step within the index range (25°–50°N, 100°–180°E) (Bradbury et al., 2002; Wang et al., 2009). The daily Northern Annular Mode (NAM) index is calculated by projecting daily geopotential height anomalies onto the leading mode of the empirical orthogonal function of daily geopotential height.

The Rossby wave source and the propagations of wave trains are adopted to reveal the circumstances and physical mechanisms related to the subseasonal reversal of temperature over NEC in winter 2014/2015, as well as the connections to the Arctic sea ice. The functions are as follows:

(1) Rossby Wave Source (RWS):

$$S = -V_\chi \cdot \nabla\zeta - \zeta D$$

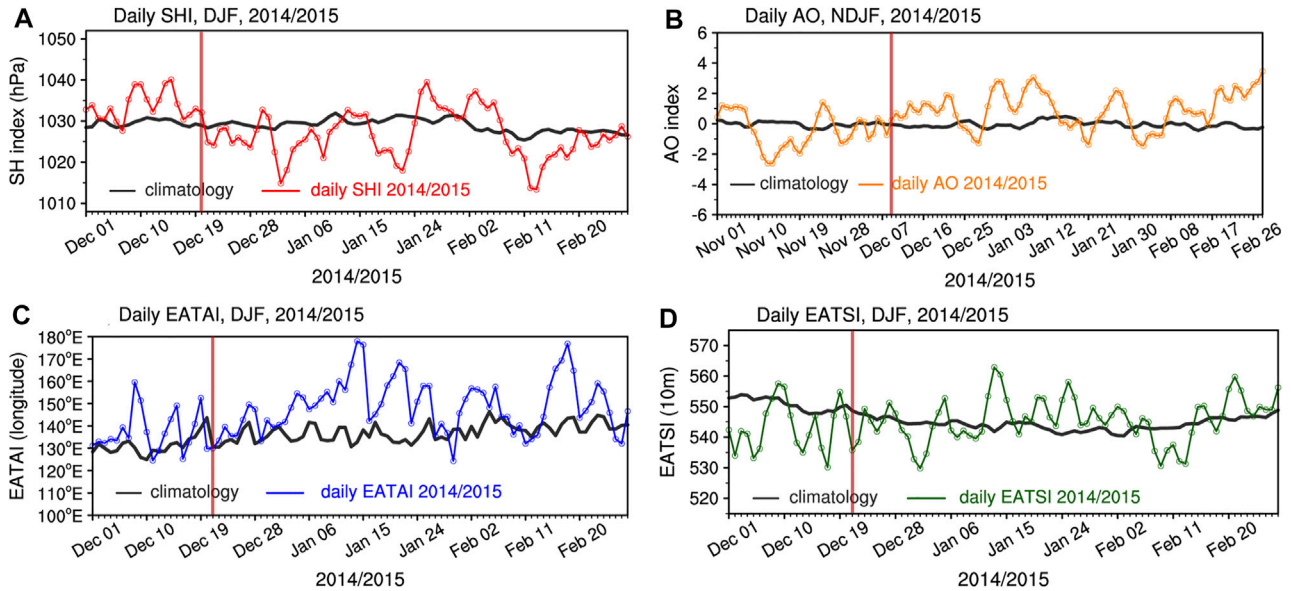

FIGURE 2 | Time series of daily indices: **(A)** intensity of the Siberian high; **(B)** AO; and **(C)** the location of the axis and **(D)** intensity of the EAT.

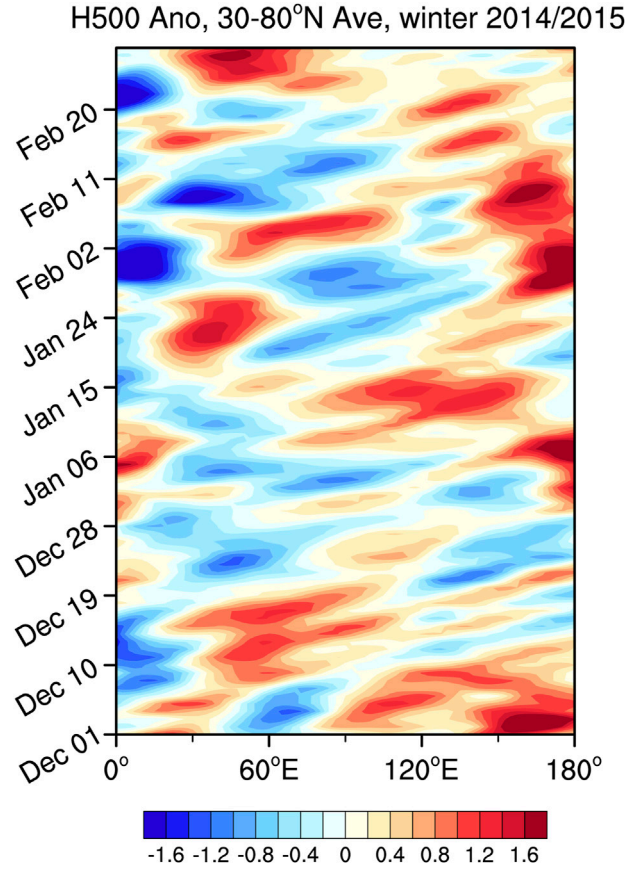

FIGURE 3 | Time–longitude cross-section of 500 hPa geopotential height (unit: 100 m) averaged between 30°N and 80°N in winter 2014/2015.

where S represents the RWS, V_χ denotes the horizontal velocity, ζ is the absolute vorticity, and D is the divergence (Sardeshmukh and Hoskins, 1988).

(2) Wave Activity Flux (WAF):

To diagnose the stationary wave propagation in the troposphere, the horizontal component of WAF generalized by Takaya and Nakamura (2001) is applied:

$$W_x=\frac{p}{2a^2|U|}\left\{\frac{U}{\cos\phi}\left[\left(\frac{\partial\psi'}{\partial\lambda}\right)^2-\psi'\frac{\partial^2\psi'}{\partial\lambda^2}\right]+V\left[\frac{\partial\psi'}{\partial\lambda}\frac{\partial\psi'}{\partial\phi}-\psi'\frac{\partial^2\psi'}{\partial\lambda\partial\phi}\right]\right\},$$

$$W_y=\frac{p}{2a^2|U|}\left\{U\left[\frac{\partial\psi'}{\partial\lambda}\frac{\partial\psi'}{\partial\phi}-\psi'\frac{\partial^2\psi'}{\partial\lambda\partial\phi}\right]+V\cos\phi\left[\left(\frac{\partial\psi'}{\partial\phi}\right)^2-\psi'\frac{\partial^2\psi'}{\partial\phi^2}\right]\right\},$$

where p = (pressure/1,000 hPa), a is the Earth's radius (unit: km), $U = (U, V, 0)^T$ denotes a steady zonally inhomogeneous basic flow, ψ' is the perturbation geostrophic stream function, and (ϕ, λ) are latitude and longitude, respectively.

The vertical component of WAF is also used to diagnose the troposphere–stratosphere interaction. The calculations are based on the functions proposed by Plumb (1985):

$$F_z=\frac{2p\Omega^2\sin^2\phi}{N^2a}\left(\frac{\partial\psi'}{\partial\lambda}\frac{\partial\psi'}{\partial z}-\psi'\frac{\partial^2\psi'}{\partial\lambda\partial z}\right)$$

where Ω is the angular velocity of rotation, N is the buoyancy frequency, and $z = -H\ln p$, where H is a constant scale height (H = 8,000 in this paper).

Moreover, the Fourier transform is also applied in this paper to isolate the wavenumbers.

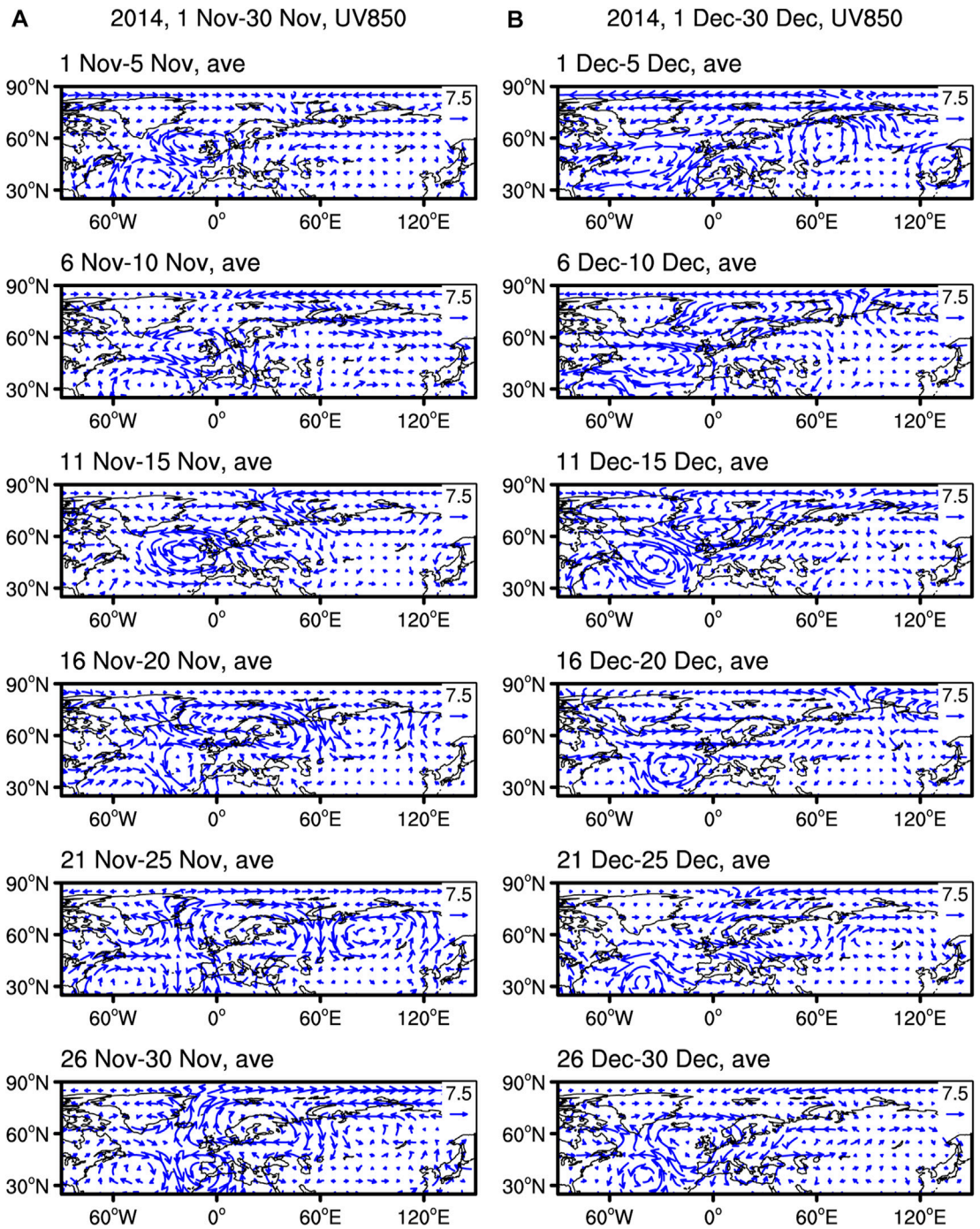

FIGURE 4 | Anomalies of horizontal wind at 850 hPa (unit: m s^{-1}) for each pentad in **(A)** November and **(B)** December 2014.

RESULTS

Daily Evolutions of Atmospheric Systems Related to NEC Temperature in Winter 2014/2015

Despite the warmer condition over NEC in winter 2014/2015, the temperature featured a significant subseasonal reversal around 22–23 December 2014, which was cooler than normal in December but anomalously warmer in January and February (**Figure 1**; hereafter abbreviated as $NECTA_{-++}$). The temperature difference at the monthly scale between January and December exceeded 3°C (**Figure 1E**). Correspondingly, the strength of the EAWM also changed around 22–23 December 2014 (figures not shown).

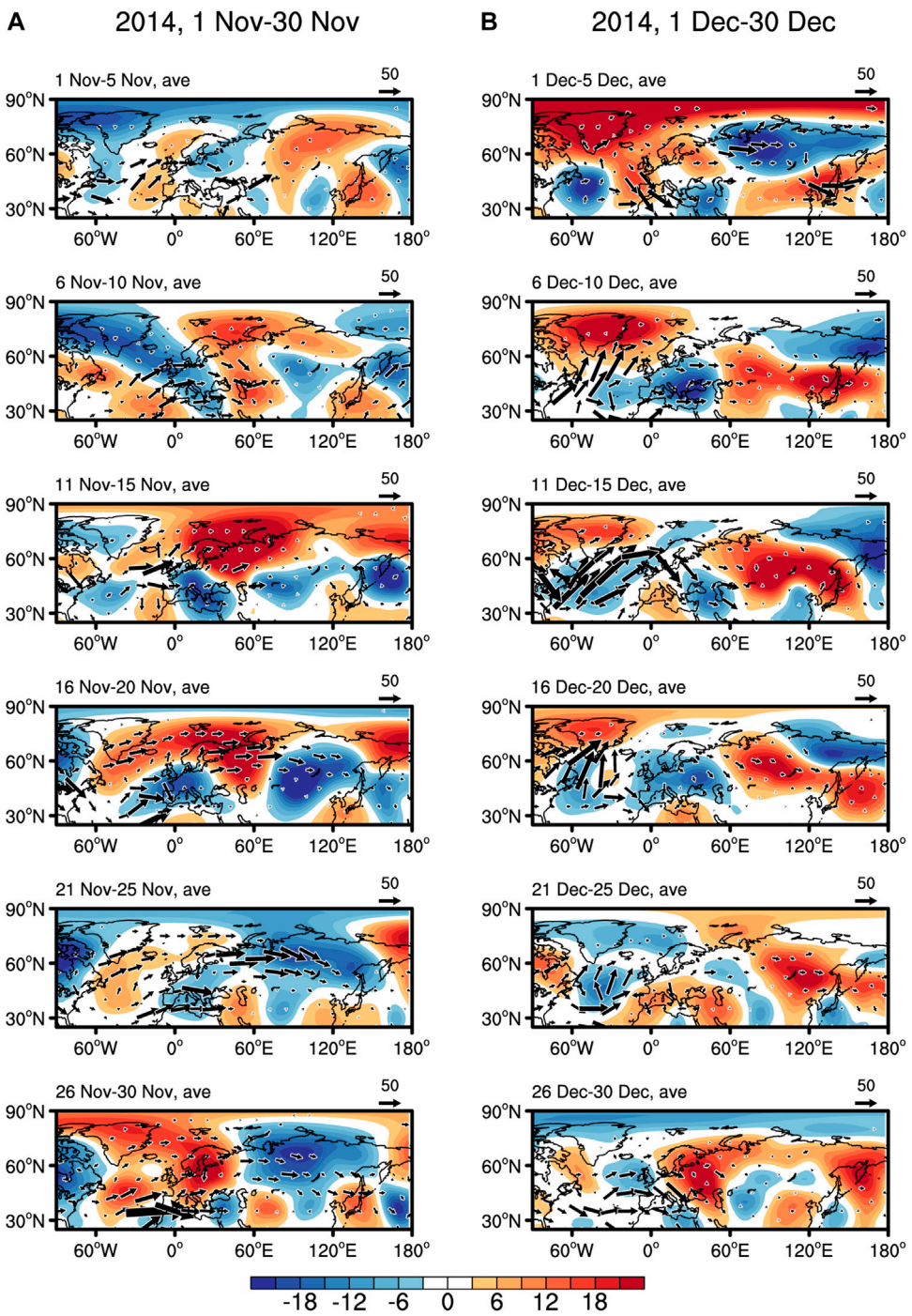

FIGURE 5 | As in **Figure 4** but for the anomalies of horizontal WAF (arrows; unit: $m^2\ s^{-2}$) and geopotential height (shading; unit: 10 m) at 500 hPa.

The time series of daily indices, including the SHI, EATSI, EATAI, and AO, are calculated to analyze the evolutions of atmospheric circulation systems related to the variations of winter temperature over NEC (**Figure 2**). The results indicate that these systems all featured subseasonal reversal in late December 2014, which is consistent with the variations of temperature over NEC. The stronger-than-normal Siberian high turned to become weakened around 20 December and sustained to February (**Figure 2A**). The invasion of cold air from the polar region to NEC is always impacted by the location and strength of the EAT. In winter 2014/2015, the EAT was stronger at the normal location during the early winter, whereas it moved eastwards and faded during the late winter (**Figures 2C,D**). Thus, the frequencies of cold surges over

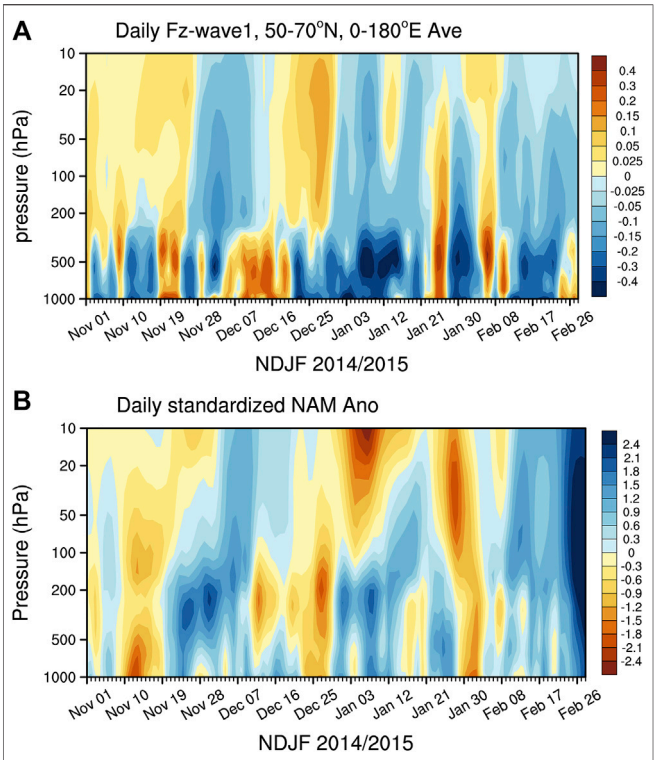

FIGURE 6 | Pressure–time cross-section of **(A)** vertical wavenumber-1 activity flux (unit: 10^{-1} m^2 s^{-2}) averaged in the domain (50°–70°N, 0°–180°E), and **(B)** standardized NAM anomalies in winter 2014/2015.

NEC decreased, favoring a warmer condition during January and February in 2015. In terms of the AO, its negative phase was maintained from November to early December, corresponding to a weakened polar vortex and lower temperature over NEC. The AO converted to a positive phase around 20 December and later strengthened significantly, thereby changing the temperature anomalies over NEC (**Figure 2B**).

Hence, the atmospheric systems related to the winter temperature over NEC all featured changes at the subseasonal scale corresponding to the subseasonal reversal of winter temperature over NEC. For further analysis, the evolutions of large-scale circulations are investigated in the next part of this paper.

Evolutionary Processes of Atmospheric General Circulations in the Mid–High Latitudes in Winter 2014/2015

The daily evolution of 500 hPa geopotential height averaged between 30°N and 80°N during winter 2014/2015 is exhibited in **Figure 3**. It indicates that the atmospheric circulations in the mid-high latitudes featured significant eastward propagation, which further affected the intraseasonal variations of the location and strength of the EAT.

Previous research has pointed out that the heat budget in the lower troposphere is the main cause of the airmass transformation of the Siberian high, and it features marked low-frequency meridional movement with a period of 10–20 days, along with the related cold-air outbreak (Ding and Krishnamurti, 1987; Ding, 1990). Staff Members of Academia Sinica (1958) concluded four categories of cold waves over East Asia and indicated the importance of eastward short waves in affecting the EAT and the Siberian high. Suda (1957) also proved that the eastward shift of the permanent trough in the mid-troposphere is responsible for the cold waves in the Far East. Some other studies have also indicated that the intraseasonal-amplification events of the winter surface Siberian high over central and western Siberia are associated with the formation of blocking bridges in the upper troposphere, which generally form as a quasi-stationary Rossby wave train propagating over the Eurasian continent (Takaya and Nakamura, 2005a; Takaya and Nakamura, 2005b). The significance of low-frequency Rossby waves and synoptic transient eddies in influencing the intraseasonal variation of the strength of the EAT were also revealed by Song et al. (2016). All these studies emphasize the critical role of the eastward wave trains over the Eurasian continent in the winter. Hence, the role of Rossby wave activities in winter 2014/2015 is discussed in the following part of this section.

An anomalous anticyclone formed in the lower troposphere over the midlatitude North Atlantic in early November 2014, and a cyclonic circulation existed to the northeast of it (**Figure 4A**). This pairing of cyclonic–anticyclonic anomalies maintained throughout December 2014 and propagated eastwards, inducing a train of cyclonic–anticyclonic circulations stretching from the North Atlantic to East Asia. The temperature over NEC decreased with the deepened EAT when the anomalous cyclones reached East Asia. However, the wind anomalies over East Asia in the lower troposphere faded from the second pentad of December 2014 and disappeared in the last pentad (12.26–12.30), corresponding to the timing of the temperature reversal (**Figure 4B**). The evolution of wind in the lower troposphere indicates the existence of eastward Rossby waves that originated from the North Atlantic and disappeared in late December 2014.

The anomalies of RWS (figures not shown), geopotential height at 500 hPa, and horizontal components of WAF (**Figure 5**) of each pentad during November–December 2014 are calculated for further investigation of the propagation of the Rossby wave train. It turns out that the RWS over the mid–high latitudes of the North Atlantic oriented east–west anomalies in November 2014, which further induced Rossby waves propagating to East Asia (**Figure 5A**). The wave train that spread from the North Atlantic to East Asia gradually weakened in early December and vanished in late December, accompanied by a faded pair of RWS anomalies during late November to early December 2014 (**Figure 5B**). Moreover, the local RWS anomalies over the Barents–Kara Sea enhanced significantly since the third pentad of November 2014, favoring the Rossby waves that originated over the North Atlantic, and then propagated to East Asia via the Barents–Kara Sea (**Figure 5A**).

Figure 5B exhibits the geopotential height anomalies over the Eurasian continent in December, which can be attributed to the Rossby waves trains that propagated from the North Atlantic to East Asia *via* the Barents–Kara Sea. Previous studies have

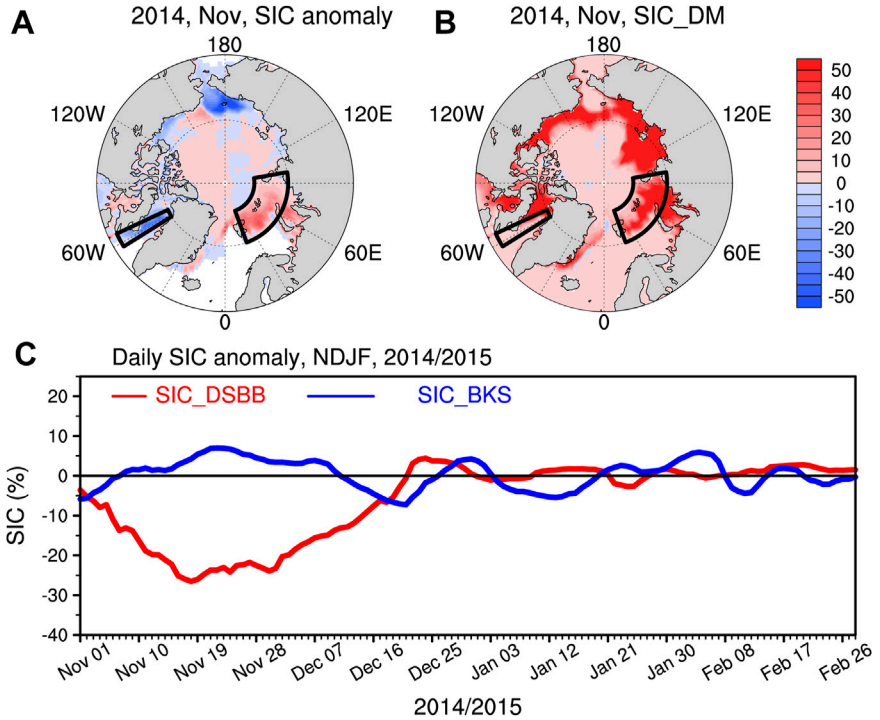

FIGURE 7 | The **(A)** anomalies and **(B)** month-to-month increments of Arctic SIC (unit: %) in November 2014. **(C)** Time series of daily SIC-DSBB and SIC-BKS anomalies.

identified that the geopotential height anomalies over the Eurasian sector are the source of the vertical development of planetary waves (Plumb, 1985; Kuroda and Kodera, 1999). Charney and Drazin (1961) discussed the propagation of the planetary waves and indicated that the wavenumber-1 and -2 components of the planetary waves dominate the vertical propagation to the stratosphere (Hayashi, 1981). Due to strong negative wind shear in the upper-stratospheric polar jet, the wave packets reflect down from the stratosphere to the troposphere, inducing the stratosphere–troposphere coupling (Kodera et al., 2013; Nath et al., 2016). In particular, zonal wavenumber-1 dominates the downward interaction on the short-term time scale (up to 12 days), forming the wavenumer-1 anomalies in the geopotential height field in the high-latitude troposphere (Perlwitz and Harnik, 2003, 2004; Shaw and Perlwitz, 2013). All these studies emphasize the importance of the wavenumber-1 component of planetary waves. Hence, the planetary wavenumber-1 component averaged over (50°–70°N, 0°–180°E) (**Figure 6A**) and the NAM index (**Figure 6B**) are calculated to analyze the daily evolutions of vertical circulations over the Eurasian continent during 1 November 2014 to 28 February 2015.

According to **Figure 6A**, the downward wave flux in the troposphere extended to the upper stratosphere throughout November 2014. This reflects the fact that the upward planetary wave flux propagating to the stratosphere was depressed, causing less wave energy reaching the stratosphere and a stronger polar vortex (**Figure 6B**). In early-to-mid December 2014, the upward propagation of wave flux in the troposphere interrupted the downward reflection of planetary wavenumber-1 from the stratosphere. However, the downward wavenumber-1 component of planetary waves dominated the troposphere in late December, strengthening the tropospheric polar vortex and causing a warmer condition over NEC. The planetary wavenumber-1 reflected downward from the stratosphere entirely ever since a minor sudden stratospheric warming occurred in early January 2015 (Manney et al., 2015). As a consequence, the polar vortex enhanced again and the geopotential height anomalies characterized the positive phase of the AO in the stratosphere. The AO pattern propagated downwards to the troposphere, enhancing the warm condition over NEC.

In conclusion, the subseasonal reversal of temperature over NEC in winter 2014/2015 was a combination of the influence of Rossby waves propagating eastwards from the North Atlantic to East Asia in November and the downward reflection of planetary wavenumber-1 from the stratosphere in mid-December 2014. The eastward Rossby waves excited by the anomalous RWS over the North Atlantic propagated through the Barents–Kara Sea in November, strengthening the Siberian high and EAT, which further favored the southward invasion of cold airmass to NEC. However, this eastward Rossby wave train gradually disappeared and slightly affected NEC in late December 2014. Meanwhile, the anomalies of the stratospheric polar vortex propagated downwards with the planetary wavenumber-1, inducing the positive phase of the AO in the troposphere and the subsequent warm condition over NEC from late December 2014.

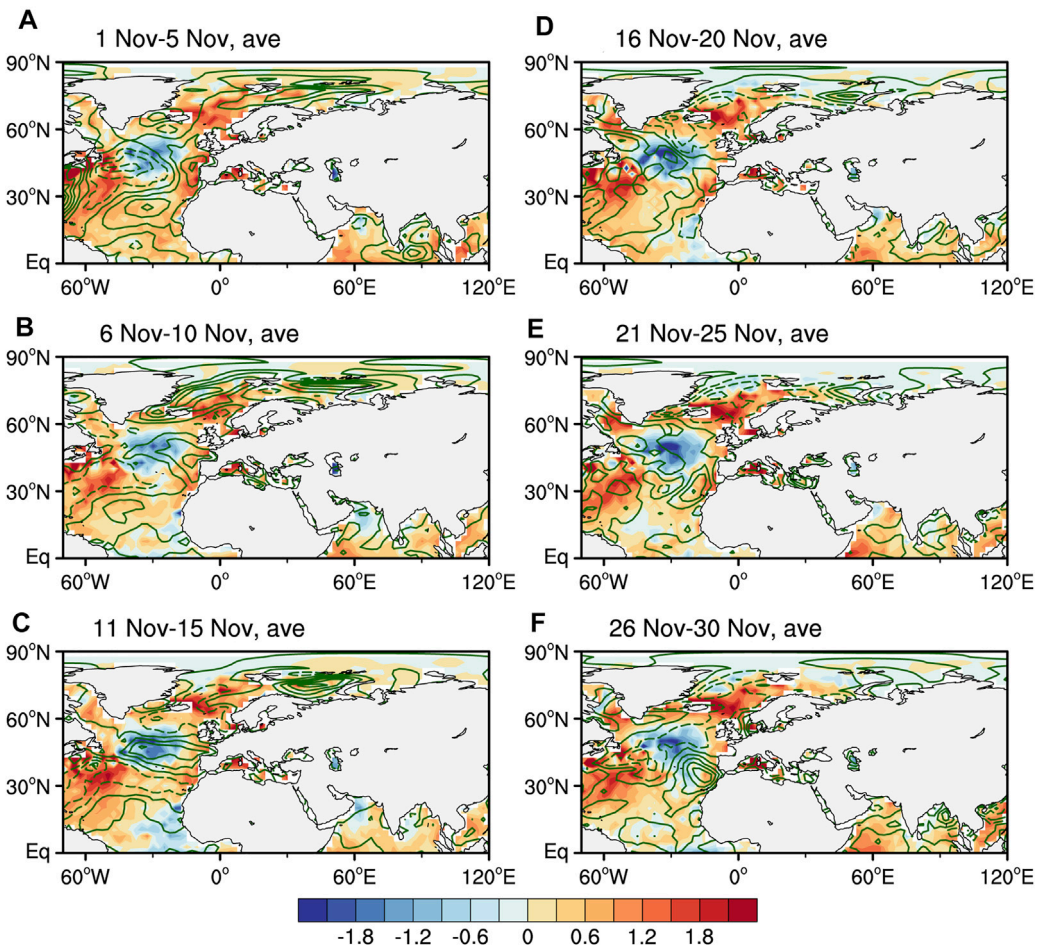

FIGURE 8 | Pentad-mean anomalies of SST (shading; unit: °C) and surface heat flux (contours; positive values denote upward heat flux; unit: 10 W m^{-2}) in November 2014.

Role of Arctic Sea Ice

The Arctic sea ice is always an essential factor for climate changes in China. Dai et al. (2019) determined the combined influences of the sea ice over the Barents–Kara Sea (SIC-BKS) and the Davis Strait–Baffin Bay (SIC-DSBB) in November to the month-to-month variability of winter temperature over NEC on the monthly scale. In this subsection, the daily impacts of the Arctic sea ice are examined based on analysis focused on the monthly variability.

The SIC was anomalously low over the Davis Strait–Baffin Bay, whereas more-than-normal SIC existed over the Barents–Kara Sea in November 2014 (**Figure 7A**). These anomalies sustained till early December and then returned to the climatology (**Figure 7C**). SIC-BKS in November increased about 40%–50% compared with that in October, which was much higher than that of SIC-DSBB (**Figure 7B**). The characteristics of SIC-BKS and SIC-DSBB indicate that the anomalies of sea ice over these two domains partly contributed to the $NECTA_{-++}$ event in winter 2014/2015, and the anomalies of SIC-BKS could have resulted in stronger circulation anomalies. The subseasonal variations of SST, RWS, and surface turbulent heat flux are analyzed to elucidate the physical mechanisms on the daily scale by which the Arctic sea ice affected the $NECTA_{-++}$ event in winter 2014/2015.

Less-than-normal SIC-DSBB in November 2014 directly induced the regionally warmer SST, and the anomalies of SST expanded to the mid–high latitudes of the North Atlantic via air–sea interactions, characterized as a tripole pattern (**Figure 8**). This tripole pattern of SST sustained throughout the whole winter of 2014/2015 (figures not shown). Correspondingly, the sea surface heat flux also featured a northeast–southwest tripole pattern over the North Atlantic (**Figure 8A**). In particular, the downward (upward) flux anomalies corresponded to the negative (positive) SST anomalies. This in-phase configuration of SST and sea surface flux was maintained in early and late November 2014 (**Figures 8A,B,E,F**), and then reversed in mid-November (**Figures 8C,D**). The local relationship between flux and SST tendency anomalies has been revealed previously (Cayan, 1992). It denotes that when flux anomalies are in-phase with SST anomalies, suggesting that flux

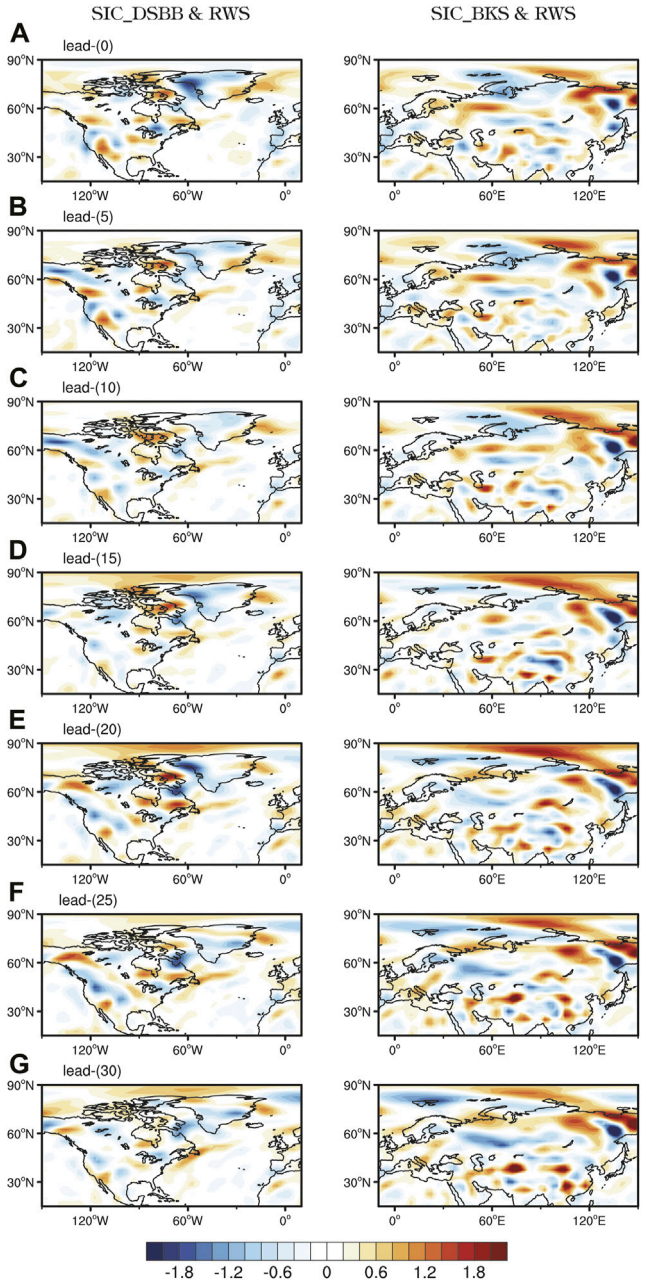

FIGURE 9 | Lag correlations between SIC indices and RWS anomalies (unit: 10^{-11} s^{-2}) in winter 2014/2015, with the interactions between SIC-DSBB and SIC-BKS removed. The left (right) column is based on SIC-DSBB (SIC-BKS).

anomalies are driven by the ocean thermal field. Therefore, in the present case, the SIC-DSBB anomalies induced the atmospheric anomalies via a direct influence on the local warming of SST in early November 2014, and these anomalies were maintained with the local air–sea interactions.

The variations and influences of SIC-BKS were different from those of SIC-DSBB. The SIC-BKS grew slightly heavier than normal in the third pentad of November 2014, inducing the local colder SST (**Figure 7C**, **Figure 8C**). The regional SST anomalies lasted and strengthened slightly till late November, corresponding to the upward sea surface heat flux. Consequently, positive anomalies of SIC-BKS caused the above atmospheric anomalies to propagate eastwards and affect the downstream circulations in late November 2014.

Since SIC-BKS and SIC-DSBB both have impacts on eastward wave trains over Eurasia, the lead–lag correlations between the RWS and SIC indices over the Barents–Kara Sea and the Davis Strait–Baffin Bay are employed to determine the differences (**Figure 9**). The SIC indices are defined as the area-averaged values over the Barents–Kara Sea and the Davis Strait–Baffin Bay. Specifically, the interactions between SIC-BKS and SIC-DSBB are removed before calculating the lead–lad correlations. The results indicate that anomalously thinner SIC-DSBB corresponded to the local pair of RWS anomalies, which sustained throughout mid-November and faded in late November 2014 (left-hand column of **Figure 9**). After excluding the influence of upstream SIC-DSBB anomalies, the anomalous RWS over the BKS could still be attributed to the heavier SIC-BKS in mid-November (right-hand column of **Figure 9**). The development of regional RWS triggered by SIC-BKS separately were corresponding to the evolutions of RWS and horizontal wave activities over Barents–Kara Sea in November 2014 (**Figure 5A**). That means the strengthened RWS over Barents–Kara Sea since the third pentad of November 2014 was excited by anomalously heavier SIC-BKS, which further intensified the eastward propagation of Rossby waves originating from the North Atlantic (**Figure 5A**; right-hand column of **Figure 9**), enhancing the atmospheric anomalies over Eurasia.

The analyses in this section can be concluded as follows: the thinner SIC-DSBB in November 2014 induced the eastward Rossby waves via regional air–sea interactions, and subsequently caused a stronger Siberian high and deepened EAT. The Rossby waves were later enhanced by heavier SIC-BKS. However, the tropospheric Rossby waves over the Eurasian section triggered by anomalous SIC-BKS and SIC-DSBB became weak and disappeared in mid-to-late December 2014. That was because of the discontinuation of SIC anomalies over the Barents–Kara Sea and the Davis Strait–Baffin Bay in early December 2014. However, the geopotential height anomalies

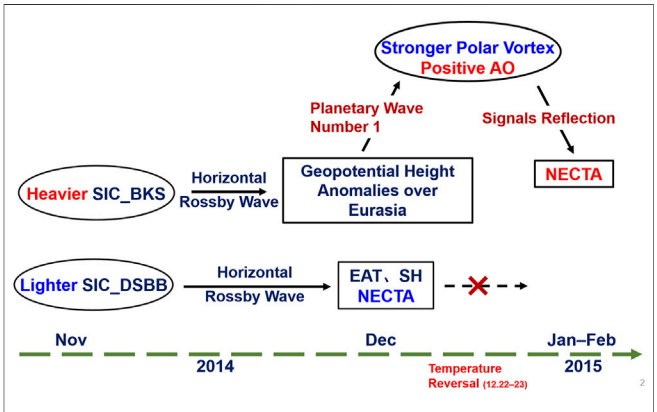

FIGURE 10 | Illustration of the factors and physical mechanisms related to the temperature reversal over NEC in winter 2014/2015.

over the midlatitudes of Eurasia due to SIC anomalies depressed the upward propagations of planetary wavenumber-1 and strengthened the stratospheric polar vortex. Later, in mid-December, the stratospheric height anomalies began to reflect downwards, causing the positive phase of the AO in the troposphere from late December.

SUMMARY AND DISCUSSION

This study gives insights into a specific event of NECTA$_{-++}$ in winter 2014/2015 on the synoptic scale. The role of Arctic sea ice in affecting the intraseasonal variations of winter temperature over NEC is further proved by examining the daily evolutions of the related atmospheric and oceanic circulations. The simplified mechanisms are shown in **Figure 10**. In short, it is a combine effect of one-month-lagged tropospheric mechanism and nearly two-months-lagged stratosphere mechanism.

The temperature of NEC and the related atmospheric circulations, like the intensity of the Siberian high, the EAT, and AO, all reversed in late December 2014. Analysis indicated that this temperature transition over NEC in winter 2014/2015 can be attributed to the combined influences of tropospheric horizontal Rossby waves in November–December 2014 and planetary waves reflected from the stratosphere since late December 2014. The anomalies of wave activity were the result of anomalous SIC-DSBB and SIC-BKS in November 2014. The regional SST and surface heat flux anomalies induced by less-than-normal SIC-DSBB in November 2014 triggered Rossby wave trains propagating eastwards to East Asia, thereby modulating the atmospheric general circulations over East Asia. Consequently, the temperature over NEC decreased with the stronger Siberian high and deeper EAT. Corresponding to heavier-than-normal SIC-BKS in November 2014, a wave train originating from the Barents–Kara Sea existed over the Eurasian sector. This wave train reinforced the eastward Rossby wave induced by SIC-DSBB anomalies and affected the temperature over NEC directly. However, the anomalies of SIC-DSBB and SIC-BKS only sustained during November 2014 and returned to normal from December 2014. Consequently, tropospheric mechanisms with which the Arctic sea ice affected the temperature of NEC were only maintained till late December 2014.

On the other hand, the response of geopotential height to this wave train was located over the Siberian sector, depressing the upward planetary wavenumber-1. The polar vortex was subsequently strengthened and the positive phase of the AO occurred in the stratosphere. Later in late December, planetary wavenumber-1 reflected downwards as stratosphere–troposphere coupling. Correspondingly, the geopotential height in the troposphere was characterized as the positive phase of the AO, favoring a warm condition over NEC from late December 2014. Thus, the temperature over NEC reversed around 22 December 2014.

This paper emphasizes the critical role of Arctic sea ice played in the subseasonal reversal of temperature over NEC in winter 2014/205. SST anomalies over the North Atlantic Sea was of great significance in this process. Previous studies also have illustrated the mechanisms by which the anomalous North Atlantic Sea SST affects general circulations over Eurasia (Zhao et al., 2019; Wu and Chen, 2020). Usually, it induces a Rossby wave-type atmospheric response propagated eastward via air-sea interaction (Chen et al., 2020). Hence, the tripole pattern of SST over the North Atlantic Sea was also essential in the formation of temperature reversal over NEC in winter 2014/2015.

DATA AVAILABILITY STATEMENT

The original contributions presented in the study are included in the article/Supplementary Material, further inquiries can be directed to the corresponding author.

AUTHOR CONTRIBUTIONS

KF proposed the idea of this study, provided insightful comments during various stages of this work and helped with editing the paper. HD analyzed the data, carried out the formal analyses, and prepared the paper.

FUNDING

This research was jointly supported by the National Natural Science Foundation of China (Grant 41730964), the Shanghai Sailing Program (Grant 21YF1452000), and the Innovation Group Project of Southern Marine Science and Engineering Guangdong Laboratory (Zhuhai) (Grant 311021001).

REFERENCES

Anderson, J. R., and Rosen, R. D. (1983). The Latitude-Height Structure of 40-50 Day Variations in Atmospheric Angular Momentum. *J. Atmos. Sci.* 40, 1584–1591. doi:10.1175/1520-0469(1983)040<1584:tlhsod>2.0.co;2

Ao, J., and Sun, J. (2016). Connection between November Snow Cover over Eastern Europe and Winter Precipitation over East Asia. *Int. J. Climatol.* 36, 2396–2404. doi:10.1002/joc.4484

Bradbury, J. A., Keim, B. D., and Wake, C. P. (2002). U.S. East Coast Trough Indices at 500 hPa and New England Winter Climate Variability. *J. Clim.* 15, 3509–3517. doi:10.1175/1520-0442(2002)015<3509:usecti>2.0.co;2

Cayan, D. R. (1992). Latent and Sensible Heat Flux Anomalies over the Northern Oceans: Driving the Sea Surface Temperature. *J. Phys. Oceanogr.* 22, 859–881. doi:10.1175/1520-0485(1992)022<0859:lashfa>2.0.co;2

Charney, J. G., and Drazin, P. G. (1961). Propagation of Planetary-Scale Disturbances from the Lower into the Upper Atmosphere. *J. Geophys. Res.* 66, 83–109. doi:10.1029/jz066i001p00083

Chen, H., Liu, L., and Zhu, Y. (2012). Possible Linkage between Winter Extreme Low Temperature Events over China and Synoptic-Scale Transient Wave Activity. *Sci. China Earth Sci.* 42, 1951–1965. doi:10.1007/s11430-012-4442-z

Chen, S., Wu, R., Chen, W., Hu, K., and Yu, B. (2020). Structure and Dynamics of a Springtime Atmospheric Wave Train over the North Atlantic and Eurasia. *Clim. Dyn.* 54, 5111–5126. doi:10.1007/s00382-020-05274-7

Dai, H., Fan, K., and Liu, J. (2019). Month-to-Month Variability of Winter Temperature over Northeast China Linked to Sea Ice over the Davis Strait-

Baffin Bay and the Barents-Kara Sea. *J. Clim.* 32, 6365–6384. doi:10.1175/jcli-d-18-0804.1

Ding, Y., and Krishnamurti, T. N. (1987). Heat Budget of the Siberian High and the Winter Monsoon. *Mon. Wea. Rev.* 115, 2428–2449. doi:10.1175/1520-0493(1987)115<2428:hbotsh>2.0.co;2

Ding, Y. (1990). Build-up, Air Mass Transformation and Propagation of Siberian High and its Relations to Cold Surge in East Asia. *Meteorol. Atmos. Phys.* 44, 281–292.

Geng, X., Zhang, W., Stuecker, M. F., and Jin, F.-F. (2017). Strong Subseasonal Wintertime Cooling over East Asia and Northern Europe Associated with Super El Niño Events. *Sci. Rep.* 7, 3770. doi:10.1038/s41598-017-03977-2

Ghil, M., and Mo, K. (1991). Intraseasonal Oscillations in the Global Atmosphere. Part I: Northern Hemisphere and Tropics. *J. Atmos. Sci.* 48, 752–779. doi:10.1175/1520-0469(1991)048<0752:ioitga>2.0.co;2

Gong, D.-Y., and Ho, C.-H. (2004). Intra-seasonal Variability of Wintertime Temperature over East Asia. *Int. J. Climatol.* 24, 131–144. doi:10.1002/joc.1006

Gong, D.-Y., Wang, S.-W., and Zhu, J.-H. (2001). East Asian Winter Monsoon and Arctic Oscillation. *Geophys. Res. Lett.* 28, 2073–2076. doi:10.1029/2000gl012311

Hayashi, Y. (1981). Vertical-zonal Propagation of a Stationary Planetary Wave Packet. *J. Atmos. Sci.* 38, 1197–1205. doi:10.1175/1520-0469(1981)038<1197:vzpoas>2.0.co;2

He, J., Lin, H., and Wu, Z. (2011). Another Look at Influences of the Madden-Julian Oscillation on the Wintertime East Asian Weather. *J. Geophys. Res.* 116. doi:10.1029/2010jd014787

Huang, R., Chen, S., Chen, W., and Hu, P. (2018). Interannual Variability of Regional Hadley Circulation Intensity Over Western Pacific during Boreal Winter and its Climatic Impact Over Asia-Australia Region. *J. Geophys. Res. Atmos.* 123, 344–366. doi:10.1002/2017jd027919

Huang, R., Chen, S., Chen, W., Yu, B., Hu, P., Ying, J., et al. (2021). Northern Poleward Edge of Regional Hadley Cell over Western Pacific during Boreal Winter: Year-To-Year Variability, Influence Factors and Associated Winter Climate Anomalies. *Clim. Dyn.* 56, 3643–3664. doi:10.1007/s00382-021-05660-9

Jeong, J.-H., Linderholm, H. W., Woo, S.-H., Folland, C., Kim, B.-M., Kim, S.-J., et al. (2013). Impacts of Snow Initialization on Subseasonal Forecasts of Surface Air Temperature for the Cold Season. *J. Clim.* 26, 1956–1972. doi:10.1175/jcli-d-12-00159.1

Jiao, Y., Wu, R., and Song, L. (2019). Individual and Combined Impacts of Two Eurasian Wave Trains on Intraseasonal East Asian Winter Monsoon Variability. *J. Geophys. Res. Atmos.* 124, 4530–4548. doi:10.1029/2018jd029953

Jin, Z., and Sun, S. (1996). The Characteristics of Low Frequency Oscillations in Winter Monsoon over the Eastern Asia. *Chin. J. Atmos. Sci. (in Chinese)* 20, 101–111.

Kalnay, E., Kanamitsu, M., Kistler, R., Collins, W., Deaven, D., Gandin, L., et al. (1996). The NCEP/NCAR 40-year Reanalysis Project. *Bull. Amer. Meteor. Soc.* 77, 437–471. doi:10.1175/1520-0477(1996)077<0437:tnyrp>2.0.co;2

Kang, L., Chen, W., Wang, L., and Chen, L. J. (2009). Interannual Variations of Winter Temperature in China and Their Relationship with the Atmospheric Circulation and Sea Surface Temperature. *Clim. Environ. Res. (in Chinese)* 14, 45–53. doi:10.3878/j.issn.1006-9585.2009.01.05

Knutson, T. R., and Weickmann, K. M. (1987). 30-60 Day Atmospheric Oscillations: Composite Life Cycles of Convection and Circulation Anomalies. *Mon. Wea. Rev.* 115, 1407–1436. doi:10.1175/1520-0493(1987)115<1407:daoclc>2.0.co;2

Kodera, K., Mukougawa, H., and Fujii, A. (2013). Influence of the Vertical and Zonal Propagation of Stratospheric Planetary Waves on Tropospheric Blockings. *J. Geophys. Res. Atmos.* 118, 8333–8345. doi:10.1002/jgrd.50650

Krishnamurti, T. N., and Gadgil, S. (1985). On the Structure of the 30 to 50 Day Mode over the Globe during FGGE. *Tellus A* 37A, 336–360. doi:10.1111/j.1600-0870.1985.tb00432.x

Kuroda, Y., and Kodera, K. (1999). Role of Planetary Waves in the Stratosphere-Troposphere Coupled Variability in the Northern Hemisphere Winter. *Geophys. Res. Lett.* 26, 2375–2378. doi:10.1029/1999gl900507

Li, W., and Tan, G. (2020). Sub-Seasonal Scale Oscillations of Winter Temperature in China and the Relationship with Interannual Anomalies. *Plateau Meteorol. (in Chinese)* 39, 110–119. doi:10.7522/j.issn.1000-0534.2019.00053

Li, J., Li, F., and Wang, H. (2020). Subseasonal Prediction of Winter Precipitation in Southern China Using the Early November Snowpack over the Urals. *Atmos. Ocean. Sci. Lett.* 13, 534–541. doi:10.1080/16742834.2020.1824547

Li, H., Fan, K., He, S., Liu, Y., Yuan, X., and Wang, H. (2021). Intensified Impacts of Central Pacific ENSO on the Reversal of December and January Surface Air Temperature Anomaly over China since 1997. *J. Clim.* 34, 1601–1618. doi:10.1175/jcli-d-20-0048.1

Liu, Y., Guo, P. W., and Feng, T. (2016). The Relationship between Winter Persistent Abnormal Low Temperature in North China and Atmospheric Lowfrequency Oscillation Activities. *Trans. Atmos. Sci. (in Chinese)* 39, 370–380. doi:10.13878/j.cnki.dqkxxb.20150314053

Lü, Z., He, S., Li, F., and Wang, H. (2018). Impacts of the Autumn Arctic Sea Ice on the Intraseasonal Reversal of the Winter Siberian High. *Adv. Atmos. Sci.* 36, 173–188. doi:10.1007/s00376-017-8089-8

Lü, Z., Li, F., Orsolini, Y. J., Gao, Y., and He, S. (2020). Understanding of European Cold Extremes, Sudden Stratospheric Warming, and Siberian Snow Accumulation in the Winter of 2017/18. *J. Clim.* 33, 527–545. doi:10.1175/jcli-d-18-0861.1

Manney, G. L., Lawrence, Z. D., Santee, M. L., Read, W. G., Livesey, N. J., Lambert, A., et al. (2015). A Minor Sudden Stratospheric Warming with a Major Impact: Transport and Polar Processing in the 2014/2015 Arctic Winter. *Geophys. Res. Lett.* 42, 7808–7816. doi:10.1002/2015gl065864

Nath, D., Chen, W., Zelin, C., Pogoreltsev, A. I., and Wei, K. (2016). Dynamics of 2013 Sudden Stratospheric Warming Event and its Impact on Cold Weather over Eurasia: Role of Planetary Wave Reflection. *Sci Rep.* 6, 24174. doi:10.1038/srep24174

Perlwitz, J., and Harnik, N. (2003). Observational Evidence of a Stratospheric Influence on the Troposphere by Planetary Wave Reflection. *J. Clim.* 16, 3011–3026. doi:10.1175/1520-0442(2003)016<3011:oeoasi>2.0.co;2

Perlwitz, J., and Harnik, N. (2004). Downward Coupling between the Stratosphere and Troposphere: The Relative Roles of Wave and Zonal Mean Processes*. *J. Clim.* 17, 4902–4909. doi:10.1175/jcli-3247.1

Plumb, R. A. (1985). On the Three-Dimensional Propagation of Stationary Waves. *J. Atmos. Sci.* 42, 217–229. doi:10.1175/1520-0469(1985)042<0217:ottdpo>2.0.co;2

Qian, W., and Zhang, W. (2007). Changes in Cold Wave Events and Warm Winter in China during the Last 46 Years. *Chinese J. Atmos. Sci. (in Chinese)* 31, 1266–1278. doi:10.3878/j.issn.1006-9895.2007.06.21

Qian, W. (2012). Physical Decomposition Principle of Regional-Scale Atmospheric Transient Anomaly. *Chinese J. Geophys. (in Chinese)* 55, 1439–1448. doi:10.6038/j.issn.0001-5733.2012.05.002

Reynolds, R. W., Smith, T. M., Liu, C., Chelton, D. B., Casey, K. S., and Schlax, M. G. (2007). Daily High-Resolution-Blended Analyses for Sea Surface Temperature. *J. Clim.* 20, 5473–5496. doi:10.1175/2007jcli1824.1

Sardeshmukh, P. D., and Hoskins, B. J. (1988). The Generation of Global Rotational Flow by Steady Idealized Tropical Divergence. *J. Atmos. Sci.* 45, 1228–1251. doi:10.1175/1520-0469(1988)045<1228:tgogrf>2.0.co;2

Shao, P. (2014). "The Characteristics of Intraseasonal Variation and the Related Atmospheric Circulation Anomalies of Winter Temperature in China from 1951 to 2013," in 31st Annual Meeting of Chinese Meteorological Society.

Shaw, T. A., and Perlwitz, J. (2013). The Life Cycle of Northern Hemisphere Downward Wave Coupling between the Stratosphere and Troposphere. *J. Clim.* 26, 1745–1763. doi:10.1175/jcli-d-12-00251.1

Sinica, S. M. O. A. (1958). On the General Circulation over Eastern Asia (II). *Tellus* 10, 58–75.

Song, L., and Wu, R. (2019a). Combined Effects of the MJO and the Arctic Oscillation on the Intraseasonal Eastern China Winter Temperature Variations. *J. Clim.* 32, 2295–2311. doi:10.1175/jcli-d-18-0625.1

Song, L., and Wu, R. (2019b). Impacts of MJO Convection over the Maritime Continent on Eastern China Cold Temperatures. *J. Clim.* 32, 3429–3449. doi:10.1175/jcli-d-18-0545.1

Song, L., Wang, L., Chen, W., and Zhang, Y. (2016). Intraseasonal Variation of the Strength of the East Asian Trough and its Climatic Impacts in Boreal Winter. *J. Clim.* 29, 2557–2577. doi:10.1175/jcli-d-14-00834.1

Song, L., Wu, R., and Jiao, Y. (2017). Relative Contributions of Synoptic and Intraseasonal Variations to Strong Cold Events over Eastern China. *Clim. Dyn.* 50, 4619–4634. doi:10.1007/s00382-017-3894-4

Suda, K. (1957). The Mean Pressure Field Characteristic to Persistent Cold Waves in the Far East. *J. Meteorol. Soc. Japan* 35A, 192–198. doi:10.2151/jmsj1923.35a.0_192

Sun, B., and Li, C. (1997). The Relationship between the Perturbations of East Asian Trough and the Tropical Convective Activities in Winter. *Chin. Sci. Bull.* 42, 500–504. doi:10.1007/bf02882851

Sun, J., Li, D., Shao, P., and Gao, N. (2019). Inter-Monthly Variation of Winter Air Temperature in China and its Relation with Atmospheric Circulation Anomalies. *Acta Meteorol. Sin. (in Chinese)* 77, 885–897. doi:10.11676/qxxb2019.050

Takaya, K., and Nakamura, H. (2001). A Formulation of a Phase-independent Wave-Activity Flux for Stationary and Migratory Quasigeostrophic Eddies on a Zonally Varying Basic Flow. *J. Atmos. Sci.* 58, 608–627. doi:10.1175/1520-0469(2001)058<0608:afoapi>2.0.co;2

Takaya, K., and Nakamura, H. (2005a). Geographical Dependence of Upper-Level Blocking Formation Associated with Intraseasonal Amplification of the Siberian High. *J. Atmos. Sci.* 62, 4441–4449. doi:10.1175/jas3628.1

Takaya, K., and Nakamura, H. (2005b). Mechanisms of Intraseasonal Amplification of the Cold Siberian High. *J. Atmos. Sci.* 62, 4423–4440. doi:10.1175/jas3629.1

Wang, L., Chen, W., Zhou, W., and Huang, R. (2009). Interannual Variations of East Asian Trough axis at 500 hPa and its Association with the East Asian Winter Monsoon Pathway. *J. Clim.* 22, 600–614. doi:10.1175/2008jcli2295.1

Wang, D., Cui, T., Si, D., Shao, X., Li, Q., and Sun, C. (2015). Features and Possible Causes for East Asian Winter Monsoon in 2014/2015. *Meteorol. Monthly* 41, 907–914. doi:10.7519/j.issn.1000-0526.2015.07.013

Wu, R., and Chen, Z. (2015). Intraseasonal SST Variations in the South China Sea during Boreal Winter and Impacts of the East Asian Winter Monsoon. *J. Geophys. Res. Atmos.* 120, 5863–5878. doi:10.1002/2015jd023368

Wu, R., and Chen, S. (2020). What Leads to Persisting Surface Air Temperature Anomalies from Winter to Following Spring over Mid- to High-Latitude Eurasia? *J. Clim.* 33, 5861–5883. doi:10.1175/jcli-d-19-0819.1

Wu, R. (2015). Coupled Intraseasonal Variations in the East Asian Winter Monsoon and the South China Sea-Western North Pacific SST in Boreal Winter. *Clim. Dyn.* 47, 2039–2057. doi:10.1007/s00382-015-2949-7

Xie, J., Zhang, M., and Liu, H. (2019). Role of Arctic Sea Ice in the 2014-2015 Eurasian Warm Winter. *Geophys. Res. Lett.* 46, 337–345. doi:10.1029/2018gl080793

Xu, X., Li, F., He, S., and Wang, H. (2018). Subseasonal Reversal of East Asian Surface Temperature Variability in Winter 2014/15. *Adv. Atmos. Sci.* 35, 737–752. doi:10.1007/s00376-017-7059-5

Yang, S., and Li, T. (2016). Intraseasonal Variability of Air Temperature over the Mid-high Latitude Eurasia in Boreal Winter. *Clim. Dyn.* 47, 2155–2175. doi:10.1007/s00382-015-2956-8

Yang, S., Wu, B., Zhang, R., and Zhou, S. (2014). Propagation of Low-Frequency Oscillation over Eurasian Mid-high Latitude in Winter and its Association with the Eurasian Teleconnection Pattern. *Chin. J. Atmos. Sci. (in Chinese)* 38, 121–132. doi:10.3878/j.issn.1006-9895.2013.12181

Yang, S., Zhu, Z., Cui, J., and Yang, Y. (2019). Regulation of the Intraseasonal Oscillation over Mid-to-high Latitude Eurasia on Winter Surface Air Temperature over China. *Dyn. Atmos. Oceans* 86, 63–72. doi:10.1016/j.dynatmoce.2019.03.003

Yao, S., Sun, Q., Huang, Q., and Chu, P. (2016). The 10-30-day Intraseasonal Variation of the East Asian Winter Monsoon: The Temperature Mode. *Dyn. Atmos. Oceans* 75, 91–101. doi:10.1016/j.dynatmoce.2016.07.001

Zhao, W., Chen, S., Chen, W., Yao, S., Nath, D., and Yu, B. (2019). Interannual Variations of the Rainy Season Withdrawal of the Monsoon Transitional Zone in China. *Clim. Dyn.* 53, 2031–2046. doi:10.1007/s00382-019-04762-9

Conflict of Interest: The authors declare that the research was conducted in the absence of any commercial or financial relationships that could be construed as a potential conflict of interest.

Publisher's Note: All claims expressed in this article are solely those of the authors and do not necessarily represent those of their affiliated organizations, or those of the publisher, the editors and the reviewers. Any product that may be evaluated in this article, or claim that may be made by its manufacturer, is not guaranteed or endorsed by the publisher.